A cyclic peptidylic inhibitor of murine urokinase-type plasminogen activator: Changing species specificity by substitution of a single residue

Lisbeth Moreau Andersen, Troels Wind, Hanne Demant Hansen, Peter A Andreasen

A cyclic peptidylic inhibitor of murine urokinase-type plasminogen activator: Changing species specificity by substitution of a single residue

Lisbeth M. ANDERSEN [1], Troels WIND, Hanne D. HANSEN, and Peter A. ANDREASEN

Department of Molecular Biology, University of Aarhus, Gustav Wieds Vej 10C, 8000 Aarhus C, Denmark

Abbreviations and trivial names used: aPC, activated protein C; BSA, bovine serum albumin; ELISA, enzyme-linked immunosorbent assay; fVIIa, factor VIIa; fXa, factor Xa; HBS, HEPES-buffered saline; HEK293T, human embryonic kidney cell line 293T; HRP, horseradish peroxidase; huPA, human uPA; IgG, immunoglobulin G; k_{on}, association rate constant; k_{off}, dissociation rate constant; K_D, equilibrium binding constant; K_i, inhibition constant; K_m, Michaelis constant; K_m^{app}, apparent K_m; muPA, murine uPA; Ni-NTA, nickel-nitrilotriacetic acid; PAB, *p*-aminobenzamidine; RU, response units; RU_{max}, maximum RU; S-2222, benzyl-IEGR-*p*-nitroaniline; S-2238, H--Pro-piperidine-Arg-*p*-nitroaniline; S-2288, H-D-IPR-*p*-nitroaniline; S-2303, *H*-D-PFR-*p*-nitroaniline; S-2366, pyro-EPR-*p*-nitroaniline; S-2403, pyro-EFK-*p*-nitroaniline; S-2444, pyro-EGR-*p*-nitroaniline; S-2765, benzyloxycarbonyl-D-RGR-*p*-nitroaniline; SDS-PAGE, sodium dodecyl sulfate polyacrylamide gel electrophoresis; Spectrozyme^{FVIIa}, methansulfonyl-D-cyclohexylalanyl-butyl-Arg-*p*-nitroaniline; SPR, surface plasmon resonance; TBS, TRIS-buffered saline; tPA, tissue-type plasminogen activator; uPA, urokinase-type plasminogen activator; uPAR, uPA receptor; V_0, reaction velocity in the absence of inhibitor; V_i, reaction velocity in the presence of inhibitor; V_{max}, maximum velocity; wt, wild type;

[1] To whom correspondence should be addressed (e-mail lma@mb.au.dk)

ABSTRACT

Urokinase-type plasminogen activator (uPA) is a potential therapeutic target in a variety of pathological conditions, including cancer. In order to find new principles for inhibiting uPA in murine cancer models, we screened a phage-displayed peptide library with murine uPA as bait. We thereby isolated several murine uPA-binding peptide sequences, the most predominant of which was the disulphide-bridged constrained sequence CPAYSRYLDC, which we will refer to as mupain-1. A chemically synthesised peptide corresponding to this sequence was found to be a competitive inhibitor of murine uPA, inhibiting its activity towards a low molecular mass chromogenic substrate as well as against its natural substrate plasminogen. The K_i value for inhibition as well as the K_D value for binding were around 400 nM. Among a variety of other murine and human serine proteases, including trypsin, mupain-1 was found to be highly selective for murine uPA and did not even inhibit human uPA measurably. The cyclic structure of mupain-1 was indispensable for binding. Alanine scanning mutagenesis identified R6 of mupain-1 as the P_1 residue and indicated an extended binding interaction including the P5, P3, P2, P1, and P1' residues of mupain-1 and the specificity pocket, the catalytic triad, and the amino acids 41, 99 and 192 located in and around the active site of murine uPA. Exchanging histidine 99 of human uPA with tyrosine, the corresponding residue in murine uPA, conferred mupain-1 susceptibility onto the latter. Peptide derived inhibitors, such as mupain-1, may provide novel mechanistic information about enzyme-inhibitor interactions, provide alternative methodologies for designing effective protease inhibitors, and be used for target validation in murine model systems.

Keywords: Proteases; Cancer; Metastasis; Phage display; Peptide

INTRODUCTION

Serine proteases of the trypsin family (clan SA) have many physiological and pathophysiological functions. There is therefore extensive interest in generating specific inhibitors to be used for pharmacological interference with their enzymatic activity. Moreover, serine proteases are classical subjects for studies of catalytic and inhibitory mechanisms (for a review, see [1]). One interesting member of the trypsin family of serine proteases is urokinase-type plasminogen activator (uPA), which catalyses the conversion of the zymogen plasminogen to the active protease plasmin through cleavage of the R15-V16 bond [2]. uPA has a catalytic serine protease domain with a trypsin-like fold. Besides the serine protease domain, uPA has an N-terminal extension consisting of a kringle domain and an epidermal growth factor domain, which binds to the cell surface-anchored uPA receptor (uPAR) [3]. uPA-catalyzed plasmin generation participates in turn-over of extracellular matrix proteins in physiological tissue remodelling (for a review, [4]). Abnormal expression of uPA is responsible for tissue damage in several pathological conditions, including rheumatoid arthritis, allergic vasculitis, and xeroderma pigmentosum. In particular, abnormal expression of uPA is a key factor for the invasive capacity of malignant tumors (for reviews, see [5, 6]).

Like with other serine proteases, there has been extensive interest in generating specific inhibitors of the enzymatic activity of uPA. The plasminogen activation activity of human uPA (huPA) can be inhibited specifically by monoclonal antibodies [7]. Several inhibitory monoclonal antibodies have epitopes encompassing the 37- and 60-loops [8]. Another type of protein protease inhibitor is the dimeric non-specific serine protease inhibitor ecotin, binding two serine protease molecules per ecotin dimer through interactions with both the protease active site and an exosite. With some success, ecotin has been converted into a high affinity human uPA inhibitor by engineering each of the two interaction sites [9]. Moreover, several classes of low molecular weight, organochemical inhibitors of human uPA have been synthesised. The binding modes for many of these were studied by X-ray crystal structure analyses. An important feature of such inhibitors is an Arg analogue inserting into the S_1 pocket of uPA. However, the challenge has been to achieve selectivity for uPA over other serine proteases with P_1 Arg specificity, by exploiting small variations in the subsite geometry of the S_1 pocket and its surroundings [10-15].

A number of murine cancer model systems are available (for a review, see [16]), and it is of great interest to use these for validation of uPA as a therapeutic target. It is a general assumption that the tumour biological function of uPA may rely on uPA produced either by the cancer cells themselves or by stromal cells. The availability of inhibitors specific for human and murine uPA, respectively, will allow evaluation of the relative importance of cancer and host uPA in xenotransplanted models with human tumours growing on immunodeficient mice. However, there is presently a lack of specific inhibitors of muPA. The only available specific inhibitors of muPA are polyclonal antibodies [17]. A series of naphtamidine-based inhibitors target to the 60-loop and $S1_\beta$ pocket of huPA had only very weak inhibitory effects on muPA [18]. A 4-amidinobenzylamine derived peptide inhibitor did inhibit rat uPA with a K_i of 19 nM, but lacked general specificity, inhibiting trypsin and uPA with almost equal potency [11]. With an inhibitor specific for murine uPA, follows a possibility to evaluate the role of uPA originating either from the host or the transplanted tumour itself.

By screening a phage-displayed peptide library with human uPA (huPA) as bait, we previously isolated a cyclic, disulphide-bridged constrained peptide, referred to as upain-1. It inhibits huPA competitively, with a K_i value of around 2 μM [19]. Site-directed mutagenesis [19] and X-ray crystal structure analysis of the upain-1-huPA complex [20] demonstrated that this peptide forms an extended interaction surface with huPA, involving not only the active site but also several surface loops. The extended interaction surface can account for the high specificity of this inhibitor, being highly selective for huPA among a number of human serine proteases. Remarkably, upain-1 did not measurably inhibit muPA [19].

With the purpose of isolating a similar inhibitor of muPA to be used in murine cancer models, we have now screened a phage-displayed peptide-library using muPA as bait. We have thereby isolated a highly specific inhibitor of muPA.

EXPERIMENTAL

Serine proteases

Active muPA was purchased from Molecular Innovation, Southfield, MI, USA. Acitive huPA was from Wakamoto Pharmaceutical Co. Ltd. Tokyo, Japan. An expression construct in the vector pcDNA3.1(-), harbouring full-length muPA, with a hexa-His tag extension at the C-terminus, was generated by standard methods from a construct kindly provided by Kasper Almholt, Finsen Laboratory, Copenhagen, Denmark. Wild-type (wt) and mutant recombinant huPA and muPA were expressed in HEK293T cells [8].

Human Glu-plasminogen and human plasmin was from American Diagnostica, Stamford, USA. Human activated protein C was from Maxygen, Hørsholm, Denmark. Human plasma kallikrein was a gift from Inger Schousboe, University of Copenhagen. Human thrombin was a gift from Dr. John Fenton, Albany, NY. Human fVIIa was from Enzyme Research, South Bend, IN, USA. Human tPA was from Genentech Inc., CA, USA. This enzyme was acquired as a mixture of one-chain and two-chain molecules and was converted to the active two-chain form with immobilised plasmin [21]. Bovine β-trypsin was from Roche Applied Sciences, Hvidovre, Denmark. It was purified from a tosyl-Phe-chloromethylketone-treated commercial preparation by chromatography on soybean trypsin inhibitor-Sepharose [22]. Murine activated protein C, murine factor IXa, murine factor Xa, murine thrombin, murine tPA, murine plasma kallikrein, and murine plasmin were purchased from Molecular Innovation, Southfield, MI, USA.

Antibodies

The monoclonal antibodies MA-H77B6 and MA-H77A10 against the A-chain of muPA were purchased from Molecular Innovation, Southfield, MI, USA. Horseradish peroxidase (HRP)-conjugated monoclonal anti-M13 phage antibody directed against the major phage coat protein g8p was from Amersham Biosciences, Hillerød, Denmark. HRP-conjugated rabbit anti-mouse IgG and HRP-conjugated swine anti-rabbit IgG was from DAKO, Denmark. Monoclonal anti-huPA antibody mAb 6 was that described before [8].

Miscellaneous materials

All enzymes used for DNA technology were from New England Biolabs, Ipswich, USA. Oligonucleotides were purchased from DNA technology, Aarhus, Denmark, or MWG Biotech AG, Germany. Expression vector pET20b(+) was from Merck Novagen, Nottingham, UK. pcDNA3.1(-) was from Invitrogen, Denmark. All DNA constructs and mutations were verified by sequencing.

The chromogenic protease substrates S-2444 (pyro-EGR-*p*-nitroaniline), S-2288 (*H*-D-IPR-*p*-nitroaniline), S-2403 (pyro-EFK-*p*-nitroaniline), S-2238 (*H*-D-Pro-piperidine-Arg-*p*-nitroaniline), S-2222 (benzyl-IEGR-*p*-nitroaniline), S-2366 (pyro-EPR-*p*-nitroaniline), S-2765 (benzyloxycarbonyl-D-RGR-*p*-nitroaniline) and S-2302 (*H*-D-PFR-*p*-nitroanline) were from Chromogenix, Mölndal, Sweden. Spectrozyme^{FVIIa} (methansulfonyl-D-cyclohexylalanyl-butyl-Arg-*p*-nitroaniline) was from American Diagnostica, Greenwich, CT. *H*-D-VLK-7-amido-4-methylcoumarin (VLK-AMC) was from Bachem, Bubendorf, Switzerland. *Para*-aminobenzamidine (PAB) and amiloride was from Sigma Aldrich, Brøndby, Denmark.

Synthetic peptides were purchased from Peptide Protein Research Ltd, Wickham, United Kingdom.

Screening of phage-displayed random peptide libraries for peptides binding to muPA

Monoclonal antibodies (5 µg/ml) against the A-chain of muPA (MA-H77B6 or MA-H77A10) were immobilised in Maxisorp Nunc-Immuno Tubes (Nunc, Roskilde, Denmark) overnight at 4°C in 0.1 M $NaHCO_3/Na_2CO_3$, pH 9.6. Nonspecific binding was blocked by incubation for 1 h at room temperature with HBS (140 mM NaCl, 10 mM Hepes pH 7.4) containing 5% skim milk powder. MuPA (200 nM) was then incubated in the tubes for 1 h at room temperature in blocking buffer, followed by 1 h incubation with 10^{11} colony-forming units from each of two phage-displayed peptide libraries, in the formats CX_7C and CX_8C, kindly provided by Dr. Erkki Koivunen, University of Helsinki, Finland. The theoretical diversity of the library was > 10^9 unique peptide inserts [23]. Subsequent to 10 washes with HBS, the bound phage particles were eluted with 1 ml of 10 mM HCl/glycin, pH 2.2. The eluted phage particles were neutralised with 0.5 ml 1 M Tris, pH 8.0, and propagated in *E. coli* JM109 cells overnight at 37°C. The bacterial cells were removed by centrifugation and the secreted phage particles were precipitated by adding 0.25 volumes 2.5 M NaCl, 20% polyethylene glycol 2000, incubation for 30 min at 0°C, and centrifugation. The pellet were resuspended in HBS with 10% glycerol. Four successive rounds of selection were performed. Alternating antibodies were used for subsequent rounds of selection in order to avoid enrichment of antibody-binding phage particles.

Expression of mupain-1 peptide sequence in fusion with the N-terminal domains of the phage coat protein g3p

A DNA fragment encoding the first two domains of the phage coat protein g3p (D1 and D2, residues 1-219) was amplified from the phage fUSE5 [24] with the PCR primers fUSEfwd (5'-CATGCCATGGGCTCGGCCGACGGGGC-3') and fUSEbck2 (5'-GTACCTCGAGGCCGCCAGCATTGACAGG-3'), using the Pfu Turbo DNA polymerase (Stratagene, La Jolla, CA, USA).The generated PCR product was purified with the Qiaquick PCR Purification kit (Qiagen, Hilden, Germany) and ligated into the *E. coli* expression vector pET20b(+) (Merck Novagen, Nottingham, UK) via NcoI and XhoI restriction sites. The resulting vector will be referred to as pETD1D2. Using the same approach, but with the mupain-1 phage as template for the PCR reaction, a vector was created for expression of the mupain-1 sequence fused to D1D2 of g3p (MGASADGACPAYSRYLDCGAAG-g3p$_{1-219}$-LEHHHHHH, the mupain-1 sequence is underlined). This fusion protein will be referred to as mupain-1-D1D2. Expression vectors for derivatives of mupain-1-D1D2 were generated by site-directed mutagenesis using pETmupain-1-D1D2 as template. The fusion proteins were expressed from cultures of *E. coli* BL21(DE3)pLysS (Merck Novagen, Nottingham, UK) containing the relevant plasmids and purified by Ni^+ chelate affinity chromatography [25, 26], subjected to size exclusion chromatography on Superdex 75 (Amersham Bioscience) equilibrated in HEPES-buffered saline (HBS, 10 mM Hepes, pH 7.4, 150 mM NaCl), and finally concentrated with Centricon Centrifugal Filter Devices (Millipore Corp., Glostrup, Denmark).

ELISA for measuring phage particles binding to muPA

Unless otherwise stated, the buffer used was HBS supplemented with 5% skim milk powder.

The relative concentration of muPA variants in conditioned medium was determined by a quantitative ELISA in which muPA was captured on Ni-NTA HisSorb™ Strips (Qiagen, Hilden, Germany) via the His_6-tag and detected with a monoclonal antibody (MA-H77B6). The procedure is otherwise as described below.

For the antibody-based ELISAs, a monoclonal antibody to be immobilised on the solid phase (2.5 µg/ml in 100 mM $NaHCO_3/Na_2CO_3$, pH 9.6) was coated in the wells of a 96-well Maxisorp plate (Nunc) followed by blocking with HBS containing 5% skim milk powder. The wells were incubated with 20 nM muPA for 1 h at room temperature. After washing with HBS, the wells were incubated with phage particles (~10^9 colony-forming units/ml) for 1 h. In some cases, up to 3 mM of PAB or amiloride were added together with the phage particles. The wells were then incubated for 1 h with a 5,000-fold dilution of HRP-conjugated anti-M13 monoclonal antibody. The wells were developed by the addition of 0.5 mg/ml *ortho*-phenylenediamine (100 µl) (KemEn Tech, Denmark) in 50 mM citric acid, pH 5.0, supplemented with 0.03% H_2O_2. When suitable color had developed, the reactions were quenched with 50 µl 1 M H_2SO_4. The A_{492} of the wells were read in a microplate reader. When testing the binding of mupain-1 phage to variants of muPA, conditioned medium from muPA-expressing HEK293T cells, was used directly in the ELISA. Each muPA variant was captured via the His_6-tag on Ni-NTA HisSorb™ Strips (Qiagen, Hilden, Germany). To ensure capture of equal amounts of the muPA variants on the solid phase, an ELISA with a monoclonal anti muPA anti-body (MA-H77B6, 1 µg/ml) instead of the phage particles and a HRP-conjugated rabbit-anti-mouse antibody (1:2000, DAKO, Glostrup, Denmark) instead of anti-M13 antibody was performed in parallel.

Determination of inhibition constant (K_i)

In order to determine the K_m^{app} and V_{max}^{app} values for S-2444 hydrolysis by muPA at varying inhibitor concentrations, 4 nM murine uPA was incubated with various concentrations of mupain-1 peptide (0-2 µM) in HBS supplemented with 0.1% BSA at 37 °C for 15 min prior to the addition of the chromogenic substrate, S-2444. Each inhibitor concentration was combined with a series of S-2444 concentrations in the range of 0-12 mM. For each inhibitor concentration ($[I_0]$), the initial velocity, monitored as an absorbance of 405 nm, were determined at several substrate concentrations. The initial velocities V were plotted versus the substrate concentrations. According to standard Michaelis-Menten kinetics, the V_{max}^{app} and the K_m^{app} values were determined at each inhibitor concentration by a nonlinear fit to the equation

$$V = (V_{max}^{app}[S]_0)/([S]_0+K_m^{app}) \quad \text{(Eq. 1)}$$

The following equation is expected to apply for competitive inhibition according to Michaelis-Menten kinetics:

$$V = ((V_{max}^{app}[S]_0)/([S]_0))+K_m(1+[I]_0/K_i) \quad \text{(Eq. 2)}$$

Here, $[S]_0$ and $[I]_0$ are the total substrate and inhibitor concentrations, respectively; K_i is the inhibition constant; K_m is the Michaelis constant for S-2444 under the assay conditions. From equation 1, one can therefore define K_m^{app} as

$$K_m^{app} = K_m(1+[I]_0/K_i) \quad \text{(Eq. 3)}$$

In the case of competitive inhibition, K_m^{app}, according to equation 2, is expected to have a linear relationship to $[I]_0$, whereas V_{max}^{app} will be independent of $[I]_0$. The K_i values can thus be estimated from the slope of the line relating K_m^{app} to $[I]_0$.

For routine determination of K_i values for the inhibition of purified recombinant protease under equilibrium inhibition conditions, a fixed concentration of the protease was preincubated in HBS with 0.1% BSA at 37°C at pH 7.4, unless otherwise stated, with various concentrations of mupain-1 peptide (0-50 μM) or mupain-1-D1D2 (0-150 μM) for 15 min prior to the addition of the appropriate chromogenic substrate. The following protease-substrate combinations were used: MuPA (4 nM) and S-2444 (750 μM); huPA (4 nM) and S-2444 (47 μM); human tPA (2.0 nM) and S-2288 (300 μM); murine tPA (2.0 nM) and S-2765 (250 μM); human plasmin (2.0 nM) and S-2403 (125 μM); murine plasmin (2.0 nM) and S-2366 (200 μM); human thrombin (0.5 nM) and S-2238 (50 μM); murine thrombin (0.5 nM) and S-2238 (100 μM); bovine β-trypsin (2.0 nM) and S-2222 (50 μM); murine β-trypsin (2.0 nM) and S-2222 (200 μM); human aPC (8.5 nM) and S-2366 (300 μM); murine aPC (8.5 nM) and S-2366 (500 μM); human fVIIa (10 nM) and Spectrozyme^{fVIIa} (500 μM); human fXa (0.5 nM) and S-2765 (100 μM); murine fXa (0.5 nM) and S-2765 (500 μM); human plasma kallikrein (4.0 nM) and S-2302 (300 μM); murine plasma kallikrein (4.0 nM) and S-2302 (125 μM); murine fIXa (5 nM) and Spectrozyme^{fIXa} (1250 μM). The initial velocities were monitored as changes in absorbance of 405 nm. As above, the K_m values for these proteases were determined by standard Michaelis-Menten kinetics. The K_i values were subsequently determined from the nonlinear regression analyses of plots for V_i/V_0 versus $[I]_0$, using an $[S]_0$ near the K_m value:

$$V_i/V_0 = (K_i([S]_0+K_m)/K_i[S]_0+K_m(K_i+[I]_0)) \quad \text{(Eq. 4)}$$

Here, V_i and V_0 are the reaction velocities in the presence and absence of inhibitor, respectively.

The K_i values for inhibition of different huPA variants by mupain-1 were determined essentially as described above except for the following modifications: 20 μl of conditioned HEK293T cell medium was used for each huPA variant instead of the purified protease and an S-2444 concentration near the K_m.

Surface plasmon resonance analysis

The equilibrium binding constants (K_D) for the binding of mupain-1-D1D2 and mupain-1 to muPA were determined by surface plasmon resonance (SPR) on a BIACORE T100 instrument (BIACORE, Uppsala, Sweden) equipped with a CM5 censor chip. Two different formats were used. In the first, an anti-muPA antibody against the A-chain (MA-H77A10) was immobilized to a density of 2000 RU/mm^2. MuPA (100 nM) in running buffer (30 mM Hepes pH 7.4, 135 mM NaCl, 1 mM EDTA) supplemented with 0.05% Tween 20 and 0.1% BSA, was injected at a flow rate of 30 μL·min^{-1} for 30 s until a capture level of ~250 RU/mm^2. Mupain-1-D1D2 or mupain-1 peptide, in various concentrations, were injected at 30 μL·min^{-1} at 25 °C in running buffer for 30 s. After discontinuation of the injection, dissociation of bound ligand was followed for another 120 s. Binding was expressed in relative response units as the response obtained from the flow cell containing immobilized ligand minus the response obtained from a reference flow cell in which the ligand (muPA) had been omitted. In the second format mupain-1-D1D2 was coupled to a density of 1000 RU/mm^2. MuPA (15 – 0.5 μM, in two-fold dilution steps in running buffer supplemented with 0.05% Tween 20 and 0.1% BSA) was injected

at a flow rate of 30 μL·min^{-1} at 25 °C for 30 s. After discontinuation of the injection, dissociation of bound ligand was followed for another 120 s. Binding was expressed in relative response units as the response obtained from the flow cell containing immobilized ligand minus the response obtained from a reference flow cell in which D1D2 has been immobilised to a density of 1000 RU/mm^2. In both formats the association rate constants (k_{on} values), the dissocation rate constants (k_{off} values), and the equilibrium binding constant (K_D) were estimated by global fitting to a 1:1 binding model, using the BIACORE T100 evaluation software.

Measurements of the binding of mupain-1 peptide variants, in which single amino acids have been substituted to Ala as well as a linear version with the Cys residues replaced by Ser, to muPA were performed as described above. However, in most of these cases the association and dissociation reactions were too fast for determination of the rate constants. The equilibrium binding constants (K_D) were therefore determined by fitting the steady state binding values to a single binding site saturation model using the equation

$$RU_{steady\ state} = (R_{max}[peptide])/(K_D+[peptide]) \qquad \text{(Eq. 5)}$$

Here, $RU_{steady\ state}$ equals steady state binding measured in RU. R_{max} is maximum binding in RU.

In order to estimate the relative binding of mupain-1 to a series of muPA variants, conditioned media from cells transfected with the corresponding muPA variant cDNA were applied to a chip at a flow rate of 30 μL·min^{-1} for 11 min. The binding of mupain-1-D1D2 to each variant was scored as the steady state binding level compared to the muPA capture level and expressed relative to the binding of mupain-1-D1D2 to muPA wt in the same experiment.

Measurements of the binding between mupain-1 peptide to variants of huPA were performed using conditioned media from cells transfected with the corresponding huPA variant cDNA. huPA was captured on the monoclonal anti-huPA antibody mAb6, immobilised on a CM5 chip to a density of ~4500 RU/mm^2. Conditioned media containing huPA was injected at a flowrate of 30 μL·min^{-1} for 120 s until a caputure level of ~950 RU/mm^2. Mupain-1 peptide in a concentration range of 0-50 μM was injected in running buffer at a flowrate of 30 μL·min^{-1} and a contact time of 30 s. After discontinuation of the injection, dissociation of bound ligand was followed for 60 s and the equilibrium binding constants (K_D) was determined by fitting the steady state binding values to a single binding site saturation model.

Investigation of substrate behaviour of mupain-1

To determine whether mupain-1-D1D2 wt behave as substrates toward closely related serine proteases, mupain-1-D1D2 was incubated at a final concentration of 2.5 μM in the presence of 50 nM bovine β-trypsin, human uPA, human aPC, human tPA, human thrombin, human fVIIa, human plasma kallikrein, human fXa, murine tPA, murine thrombin, murine plasmin, murine fIVa, murine fXa, murine plasma kallikrein and murine trypsin respectively, in HBS at 37°C for different time periods (0-120 min). The reactions were quenched by adding 0.1 volume of 0.1 M HCl. The reaction products were analysed by SDS-PAGE under reducing conditions and Coomassie Blue staining.

Plasminogen activation assay *in vitro*

MuPA (0.25 nM) was preincubated with increasing concentrations of mupain-1 (0-10 μM) in HBS containing 0.1% BSA for 15 min at 37°C. Plasminogen (0.5 μM) and the chromogenic plasmin

substrate S-2251 (500 μM) were added and the change in absorbance at 405 nm was recorded at regular intervals for a time period of 120 min.

Plasminogen activation assay in the presence of WEHI-3 cells

WEHI-3 cells, grown in Dulbecco's Modified Eagle Medium 4.5 g/l glucose supplemented with 10% fetal bovine serum, 4.5 g/l glucose, 10 U penicillin/ml, 100 μg streptomycin/ml, and 2 mM L-glutamine (Cambrex Bio Science, Verviers, Belgium), were washed extensively in PBS, and resuspended in 50 mM Tris, 100 mM NaCl, pH 7.4 (TBS) with 0.1% BSA at a density of 10^7 cells/ml. The cells were preincubated for 1 h at 37°C with 50 nM muPA, and subsequently washed to remove unbound muPA. They were then aliquoted into the wells of 96-well microtiter plates (Nunc) and preincubated for 15 minutes at room temperature with mupain-1. Plasminogen (0.5 μM) and VLK-AMC (200 μM) were added to a total volume of 200 μl. The fluorescence of the wells was monitored at 2-min intervals in a Spectromax Gemini fluorescence plate reader (Molecular Devices) using an excitation wavelength of 390 nm and an emission wavelength of 480 nm.

Stability of mupain-1 in serum

Mupain-1 (400 μM) was incubated in 77% fetal bovine serum (Cambrex Bio Science, Verviers, Belgium) or 77% mouse serum (Dako Denmark A/S, Glostrup, Denmark) at 37°C for 0, 1, 2, or 20 hours. After the incubation, 1/15 volume of 1 M glycine/HCl, pH 3, and 1/15 volume of 1 M HCl was added to inactivate α_2-macroglobulin. The acid treatment was followed by neutralisation with 4 volumes of 30 mM Hepes, pH 7.4, 135 mM NaCl, 1 mM EDTA, 0.1% BSA. Aliquots of various volumes of incubation mixture were then mixed with a fixed concentration of muPA (4 nM). The remaining activity of muPA was determined by an S-2444-assay.

RESULTS

Selection of a peptide binding to muPA

For isolating muPA binding peptides, we used a phage-displayed random peptide library with peptide sequences in the formats CX_7C and CX_8C, where X denotes random natural amino acids and the flanking cysteine residues are oxidized, resulting in constrained circular peptides. The theoretical diversity of the library was > 10^9 unique peptide inserts. As bait, we used muPA immobilised on a monoclonal anti-muPA antibody with an epitope in the A-chain. Four rounds of selection were performed. Among 24 individual phage clones showing muPA-binding in ELISA, all had sequences which were variations over a theme with a centrally placed arginine residue. One of the two most common sequences, displayed on 6 phage clones out of the 24, had the sequence CPAYSRYLDC. This sequence was chosen for further analysis and will be referred to as mupain-1. The other common sequence, CPLYNRMIGC, will be referred to as mupain-2.

The selected peptide sequence is a competitive inhibitor of muPA

A peptide corresponding to the mupain-1 sequence, with oxidized cysteines, was synthesized chemically. Also, to be able to analyse muPA-binding of the mupain-1 sequence in its native state, i.e., at the N-terminus of the phage coat protein g3p, the mupain-1 sequence was expressed in fusion with the two N-terminal domains of g3p, D1 and D2. The fusion protein will be referred to as mupain-1-D1D2.

The mupain-1 peptide and mupain-1-D1D2 inhibited the peptidolytic activity of muPA against the chromogenic substrate S-2444, while the fusion partner D1D2, without the mupain-1 sequence, showed no or only weak inhibitory activity, as no inhibition could be measured with D1D2 concentrations up to 150 μM. By determining the rate of S-2444 hydrolysis at several substrate and several inhibitor concentrations, an apparent K_m (K_m^{app}) could be determined at each inhibitor concentration. The K_m^{app} increased linearly with the inhibitor concentration, while V_{max}^{app} changed only negligibly (Table 1), clearly in agreement with the expected inhibition mode of a competitive inhibitor (Equation 3). We therefore concluded that mupain-1 competitively inhibits muPA.

In our analysis of inhibition kinetics, we routinely used plots of V_i/V_0 versus inhibitor concentration at a single substrate concentration near the K_m value, and analysis by non-linear regression curve-fitting according to Equation 4 and independently determined K_m values for muPA-catalysed S-2444 hydrolysis.

The K_i value for inhibition of muPA by the mupain-1-D1D2 construct was significantly higher (10 fold) than the corresponding values for the chemically synthesized peptide, suggesting that presentation of the peptide sequence in a protein scaffold considerably changed the affinity for the muPA target.

The K_i value did not depend on pH (data not shown).

Mupain-1 inhibits muPA-catalysed activation of plasminogen *in vitro* and on cell surfaces

The effect of mupain-1 on the plasminogen activation activity of muPA was tested in a coupled plasminogen activation assay. MuPA was incubated with the peptide prior to the addition of plasminogen and a chromogenic substrate for plasmin (S-2251). Figure 1A illustrates how increasing amounts of mupain-1 inhibit the plasminogen activation activity of muPA in a dose dependent manner.

The effect of mupain-1 on the plasminogen activation activity of muPA bound to uPAR on the surface of murine myelomonocytic WEHI-3 cells was determined by a coupled plasminogen activation assay. Aliquots of WEHI-3 cell suspension (10^7 cells/ml) that had been saturated with muPA were incubated at room temperature for 15 minutes without addition or in the presence of increasing amounts of mupain-1. Cells without muPA served as a negative control. Plasminogen and the fluorogenic plasmin substrate VLK-AMC were added to start the reaction and fluorescence was measured over time. Mupain-1 was found to inhibit the uPAR-bound muPA-catalysed plasminogen activation on the cell surface in a dose dependent manner (Figure 1B).

The equilibrium binding constant for mupain-1-D1D2 and mupain-1 peptide binding to muPA

The equilibrium binding constant, K_D, for the binding of mupain-1-D1D2 and mupain-1 peptide to muPA was determined using SPR with a BIACORE T100 instrument (Table 2). In one format, muPA was immobilised on a CM5 chip via a monoclonal anti-muPA antibody with an epitope in the muPA A-chain. The fusion protein (Figure 2A) or the peptide (Figure 2B) was injected in various concentrations. The rate constants for association and dissociation of the muPA-mupain-1-D1D2 complex and the muPA-mupain-1 complex were estimated by global fitting with BIACORE T100 Evaluation Software, assuming a simple 1:1 binding model. The K_D values were then calculated as the k_{off}/k_{on} ratios. The estimated K_D values agree excellently with K_i values from the enzyme kinetic measurements (see above). Using an alternative format, in which mupain-1-D1D2 was immobilised on the chip and muPA injected, the same K_D value was found as with immobilised muPA, although the rate constants differed somewhat.

Determination of the protease specificity for mupain-1

We determined K_i values for the inhibition of several other related murine and human clan SA serine proteases that prefer a basic P_1 residue, using mupain-1 peptide in competitive chromogenic substrate assays, each one with the corresponding optimal substrate for the respective protease. We observed no inhibition of murine or human tPA, activated protein C, plasmin, thrombin, plasma kallikrein, fVIIa, fIXa, and fXa by mupain-1 even at the highest concentrations tested, 150 μM. If one then assumes a lower limit for detection of approximately 10% inhibition, we estimate, on the basis of Equation 4, the K_i values for inhibition of these proteases. Mupain-1 inhibited β-trypsin with a K_i value 50 - 100 fold higher than that for muPA (Table 3). To further characterise the interaction of mupain-1 with uPA-related proteases, we investigated whether any of the tested proteases were able to cleave the mupain-1 sequence. Mupain-1-D1D2 (2.5 μM) was incubated with individual proteases (50 nM) at 37°C for the time period 0-120 min, and the reaction products were analysed by SDS-PAGE. Under these conditions none of the tested proteases were able to cleave mupain-1 (data not shown).

Effect of active site reagents on the mupain-1-muPA binding

PAB and amiloride contain an amidino- or a guanidino group, respectively, that insert into the S1 pocket in the active site of muPA. To investigate whether mupain-1 binds muPA via interaction in the S1 pocket, the ability of PAB and amiloride to displace mupain-1-phage particles from murine uPA was determined by a phage-ELISA. The experiments showed that both PAB and amiloride are capable of displacing mupain-1 phage particles in a dose dependent manner suggesting overlapping binding sites between mupain-1 and the two chemical compounds (data not shown).

Mutagenesis of residues in the mupain-1 sequence

In order to evaluate the importance of individual residues in mupain-1 for the binding to muPA, all the residues (except Ala3) were independently substituted by Ala, either as a chemical peptide or in the mupain-1-D1D2 background. A linear variant with the N- and C-terminal cysteine residues replaced by serine residues was also constructed.

The effect of these substitutions on the inhibitory properties of the mupain-1 sequence was measured, using plots of V_i/V_0 versus inhibitor concentration at a single substrate concentration near the K_m value. Likewise, we measured the binding affinity by the use of SPR, using the steady state binding levels at several different peptide concentrations as the association and dissociation kinetics were too fast to allow determination of the rate constants (Table 4). The results obtained by the two types of analyses agreed well. The analyses demonstrated that substitution of P2, Y4, S5, R6, and Y7 resulted in a strongly decreased affinity for muPA, while substitution of L8 or D9 had little or no effect. Furthermore, the Cys residues in positions 1 and 10, and therefore the cyclical nature of the peptide sequence, were found to be necessary for binding. Upain-1, a cyclic peptide, which inhibits huPA competitively, inhibited muPA very poorly, with a K_i value 200-fold higher than that for inhibition by mupain-1.

Mapping of the binding site for mupain-1 on uPA by alanine-scanning mutagenesis

To describe the binding interface for mupain-1 on muPA, we used site-directed mutagenesis of muPA expressed recombinantly in HEK293T cells. Principally, the alanine substitutions were chosen on the basis of a three dimensional model of muPA aligned with the upain-1-uPA crystal structure [20]. Residues in muPA closer than 5 Å to and pointing toward upain-1 in this model were decided to be of particular interest in relation to the binding of mupain-1 to muPA, assuming that mupain-1 and upain-1 have similar binding sites. In order to estimate the binding of the muPA variants relative to the binding of the wt, we used a phage particle ELISA and a BIACORE setup, in both cases employing directly conditioned media from transfected HEK293T cells. In the ELISA, the muPA variants from the conditioned media were captured in Ni-NTA coated wells and the relative binding of phage particles subsequently scored, using a control in which the capture levels of the various variants were estimated with a monoclonal anti-muPA antibody (Figure 3A). In the BIACORE, the muPA variants from the conditioned media were captured on a monoclonal anti-muPA antibody which was immobilised on a CM5 chip, and the binding of mupain-1-D1D2 to captured muPA recorded (Figure 3B).

A more than 5-fold reduction in mupain-1 binding was found for the following mutants: K41A, H57A, Y99A, D189A, S195A, whereas the substitutions Q35A, Q60A, K143A, E146A, and R217A had no or very moderate influence on the binding of mupain-1. In addition, the mutant K15A, introduced to ensure that the protein remained in the inactive pro-enzyme form, reduced the binding of mupain-1 to unmeasurably low levels (Figure 3). For unknown reasons, the mutant Q192A could not be expressed and the importance of this residue in binding of mupain-1 has therefore not been elucidated.

Changing the susceptibility of huPA to mupain-1

By combining the biochemical data and the structural information given by a sequence alignment of the protease domain of huPA and muPA, we identified two amino acids (K41 and Y99) in

muPA which are highly important for the binding of mupain-1 and which are not conserved beween huPA and muPA. Even though the importance of Q192 of muPA could not be tested by alanine substitution, it may, according to a three-dimensional model of muPA, be located in the binding area of mupain-1, and this residue is also not conserved between huPA and muPA. In an attempt to confer mupain-1 sensitivity to huPA, we decided to graft the residues present at position 41, 99 and 192 in muPA onto huPA. In order to evaluate the importance of individual amino acids on the species specificity, we produced seven huPA mutants which combined the mutations at the three positions in all possible ways, *i.e*., three single mutants, three double mutants, and one triple mutant. The K_m and V_{max} values for S-2444 hydrolysis by the different huPA variants were determined using the conditioned media from HEK293T cells transfected with the corresponding cDNAs. The huPA variants were tested for binding to mupain-1 in SPR binding analysis. We found that binding between mupain-1 peptide and huPA wt, huPA V41K, huPA Q192K, and huPA V41K-Q192K was below measurable levels with concentration of mupain-1 of 50 µM. However, the huPA variants H99Y, V41K-H99Y, H99Y-Q192K, and V41K-H99Y-Q192K showed clear binding to mupain-1 in the SPR binding analysis and the K_D values for the binding between mupain-1 and these variants are listed in Table 5. Substituting the histidine residue at position 99 with a tyrosine greatly enhanced the binding of mupain-1 to huPA, resulting in a K_D of 12.0 µM. A tyrosine at position 99 combined with a lysine at position 192 did not further enhance the binding to mupain-1. However, combining the tyrosine at position 99 with lysine at position 41 enhanced the binding to mupain-1 2-fold compared with the single substitution at position 99. The affinity between mupain-1 and huPA is further enhanced by grafting all three amino acids at position 41, 99, and 192 in muPA onto huPA; we hereby obtained a K_D value of 4.2 µM, only approximately 10-fold higher than the corresponding value for the binding of mupain-1 to muPA (Table 5). The K_i values for inhibition of the different huPA variants by mupain-1 were determined using the conditioned media and a single substrate concentration near the K_m value. When no inhibition was observed even at the highest concentration tested (100 µM) a Ki value was estimated on the basis of Equation 4, assuming a lower limit for detection of approximately 10% inhibition. In excellent agreement with the K_D values, the single substitution at position 99 resulted in a K_i of 15.3 µM, while combining this substitution with a substitution at position 41 further decreased the K_i to 6.9 µM. The largest effect on K_i was again observed when grafting all three amino acids from muPA onto huPA resulting in a K_i of 3.6 µM which again is around 10-fold higher compared to the same value determined for muPA. The K_m value for hydrolysis of S-2444 was also markedly influenced by substitution of amino acids on the before mentioned positions in huPA. The K_m value for the triple mutant of huPA was comparable to the corresponding value obtained for muPA wt (Table 5).

The stability of mupain-1 in serum

The ability of certain amounts of mupain-1 to inhibit muPA changed little if at all, whether it was assayed directly or after having been incubated for 20 hours with serum (Figure 5). The change observed corresponded maximally to an approximately 50% loss of inhibitory active peptide during the incubation.

DISCUSSION

In this report, we describe the isolation of mupain-1, a muPA binding peptide from a phage-displayed library of disulphide-bridged constrained peptides. The peptide, of the format CX_8C, is a competitive inhibitor of muPA. It displayed a K_i for inhibition and a K_D for binding of approximately 400 nM. It is highly specific for muPA. The affinity for almost all tested serine proteases were several hundred-fold higher than for muPA. The one exception was β-trypsin, which was inhibited with a 50-fold lower efficiency. Strikingly, mupain-1 did not measurably bind to huPA, having a K_i for inhibition by mupain-1 more than 2500-fold higher than muPA. Mupain-1 expressed in fusion with the N-terminal domains, D1 and D2, of the phage coat protein g3p had markedly lower affinity that the synthetic peptide. This observation is remarkable since a previous study with a peptide of similar format, binding to huPA, showed higher affinity for its target when fused to D1D2 [19].

We undertook a partial mapping of the mupain-1 binding site of muPA by alanine substitution mutagenesis and in this way identified 5 residues of importance for binding. Three of these, H57, D189, and S195, are part of the actual active site. H57 and S195 are parts of the catalytic triad and D189 are localised at the bottom of the specificity pocket. The importance of these residues is in agreement with the fact that mupain-1 is a competitive inhibitor. In addition, K41 and Y99 were also shown to be important for binding, showing that mupain-1 also targets areas flanking the actual active site. When planning the alanine substitution mutagenesis, we also suspected Q192 of being involved in mupain-1 binding, but were unable to express this variant.

The high specificity of mupain-1 for muPA can be explained, at least in part, by the binding to these residues, as different residues are present in these positions in the other serine proteases tested (Table 6). In particular, there is a striking specificity of mupain-1 for muPA over huPA. Likewise, we previously isolated a peptide sequence, upain-1, CSWRGLENHRMC, a competitive inhibitor of huPA, but with very low affinity to muPA [19]. In both cases, the species specificity is likely to rely on binding to loops outside the actual active site, such as the 37, 60, and 99 loops. But it should be noted that differences between murine and human uPA must also exist within the actual active site. Although the activation loop in both man and mouse plasminogen is CPGRVVGGC, the K_m value for S-2444 hydrolysis by muPA and huPA is about 10-fold higher for muPA than for huPA (Table 4). In order to provide further information about the basis for this specificity, we grafted the residues present in positions 41, 99, and 192 of muPA onto huPA. The triple mutant of huPA, having its natural residues replaced by the counterparts from muPA, had a K_m value for S-2444 hydrolysis comparable to that of muPA wt. Moreover, the binding affinity for mupain-1 increased more than 400-fold by the triple substitution, and the K_i was only 10-fold higher than that for wt muPA. This increase in affinity for mupain-1 was mainly contributed by the H99Y substitution, which causes an at least 100-fold increase in affinity. Residue number 99 are localised in the 99-loop, which lines the S_2 pocket. This position has previously been implicated in determining the substrate specificity of factor VIIa [27]. His99 also played a role in the recognition of upain-1 by uPA.

We undertook a comprehensive alanine scanning mutagenesis of mupain-1 and found that the cyclic structure as well as residues P2, Y4, S5, R6, and Y7 were of decisive importance for the affinity to muPA, while L8 and D9 could be substituted with Ala without affecting the affinity to muPA. Since

R6 is the only arginine residue, it must be the P_1 residue and insert into the specificity pocket. Accordingly, S5 will have to be the P_2 residue and Y4 the P_3 residue, while Y7 must be the P_1' residue. L8 and D9 are likely to point away from the muPA surface.

Peptidylic inhibitors selected from phage displayed libraries provide generally applicable tools for studying protease specificity and inhibitory and catalytic mechanisms (for a review, see [28]). Why is mupain-1 an inhibitor, and not a substrate? We previously asked the same question in the case of upain-1, the inhibitor of huPA. The three-dimensional structure of upain-1-uPA complex [20] showed that the bulky Trp residue in the P2 position is too large to be accommodated in the narrow P2 binding site of uPA. The proper alignment of the scissile bond into the active site is therefore not possible. Instead, the side chain of the Glu residue in position 7 of upain-1 bends into the oxyanion hole and further prevents hydrolysis. A similar mechanism may be predicted in the case of mupain-1, which has a Ser in the P2 position, also likely to be too large for the P2 binding site of muPA.

It seems that peptide-based drugs are now realistic alternatives to other biopharmaceuticals such as antibodies. Most of the past limitations to peptides have been removed by new technologies. Phage-display technologies can provide novel peptides that bind protein targets with high affinity and specificity (for a review, see [29]). Peptides have specificities comparable to that of monoclonal antibodies and protein protease inhibitors, but at the same time a size eventually allowing for chemical synthesis and modification. Clearance rates may be reduced by derivatisation with polyethylene glycol. In the case of mupain-1, we already demonstrated that the peptide is stable in serum. After appropriate affinity maturation and perhaps incorporation of unnatural amino acids, mupain-1 may become a useful high-affinity inhibitor of muPA in murine models of tumour invasion and metastasis.

ACKNOWLEDGMENTS

The technical assistance Anni Christensen is gratefully acknowledged. This work was supported by grants from the Danish Cancer Society, the Danish Cancer Research Foundation, the Danish Research Agency, the Carlsberg Foundation, the Novo-Nordisk Foundation, and European Union FP6 contract LSHC-CT-2003 h503297 (the Cancer Degradome) to PAA.

REFERENCES

1 Hedstrom, L. (2002) Serine protease mechanism and specificity. Chem. Rev. **102**, 4501-4524

2 Barret, A. J., Rawlings, N. D. and Woessner, J. F. (1998) Handbook of Proteolytic Enzymes. Academic Press, London

3 Dano, K., Moller, V., Ossowski, L. and Nielsen, L. S. (1980) Purification and characterization of a plasminogen activator from mouse cells transformed by an oncogenic virus. Biochim. Biophys. Acta. **613**, 542-555

4 Dano, K., Andreasen, P. A., Grondahl-Hansen, J., Kristensen, P., Nielsen, L. S. and Skriver, L. (1985) Plasminogen activators, tissue degradation, and cancer. Adv. Cancer Res. **44**, 139-266

5 Andreasen, P. A., Egelund, R. and Petersen, H. H. (2000) The plasminogen activation system in tumor growth, invasion, and metastasis. Cell. Mol. Life Sci. **57**, 25-40

6 Andreasen, P. A., Kjoller, L., Christensen, L. and Duffy, M. J. (1997) The urokinase-type plasminogen activator system in cancer metastasis: a review. Int. J. Cancer **72**, 1-22

7 Kaltoft, K., Nielsen, L. S., Zeuthen, J. and Dano, K. (1982) Monoclonal antibody that specifically inhibits a human Mr 52,000 plasminogen-activating enzyme. Proc. Natl. Acad. Sci. U S A **79**, 3720-3723

8 Petersen, H. H., Hansen, M., Schousboe, S. L. and Andreasen, P. A. (2001) Localization of epitopes for monoclonal antibodies to urokinase-type plasminogen activator: relationship between epitope localization and effects of antibodies on molecular interactions of the enzyme. Eur. J. Biochem. **268**, 4430-4439

9 Laboissiere, M. C., Young, M. M., Pinho, R. G., Todd, S., Fletterick, R. J., Kuntz, I. and Craik, C. S. (2002) Computer-assisted mutagenesis of ecotin to engineer its secondary binding site for urokinase inhibition. J. Biol. Chem. **277**, 26623-26631

10 Mackman, R. L., Katz, B. A., Breitenbucher, J. G., Hui, H. C., Verner, E., Luong, C., Liu, L. and Sprengeler, P. A. (2001) Exploiting subsite S1 of trypsin-like serine proteases for selectivity: potent and selective inhibitors of urokinase-type plasminogen activator. J. Med. Chem. **44**, 3856-3871

11 Schweinitz, A., Steinmetzer, T., Banke, I. J., Arlt, M. J., Sturzebecher, A., Schuster, O., Geissler, A., Giersiefen, H., Zeslawska, E., Jacob, U., Kruger, A. and Sturzebecher, J. (2004) Design of novel and selective inhibitors of urokinase-type plasminogen activator with improved pharmacokinetic properties for use as antimetastatic agents. J. Biol. Chem. **279**, 33613-33622

12 Spencer, J. R., McGee, D., Allen, D., Katz, B. A., Luong, C., Sendzik, M., Squires, N. and Mackman, R. L. (2002) 4-Aminoarylguanidine and 4-aminobenzamidine derivatives as potent and selective urokinase-type plasminogen activator inhibitors. Bioorg. Med. Chem. Lett. **12**, 2023-2026

13 Sperl, S., Jacob, U., Arroyo de Prada, N., Sturzebecher, J., Wilhelm, O. G., Bode, W., Magdolen, V., Huber, R. and Moroder, L. (2000) (4-aminomethyl)phenylguanidine derivatives as nonpeptidic highly selective inhibitors of human urokinase. Proc. Natl. Acad. Sci. U S A **97**, 5113-5118

14 Wendt, M. D., Rockway, T. W., Geyer, A., McClellan, W., Weitzberg, M., Zhao, X., Mantei, R., Nienaber, V. L., Stewart, K., Klinghofer, V. and Giranda, V. L. (2004) Identification of novel binding interactions in the development of potent, selective 2-naphthamidine inhibitors of urokinase. Synthesis, structural analysis, and SAR of N-phenyl amide 6-substitution. J. Med. Chem. **47**, 303-324

15 Zeslawska, E., Jacob, U., Schweinitz, A., Coombs, G., Bode, W. and Madison, E. (2003) Crystals of urokinase type plasminogen activator complexes reveal the binding mode of peptidomimetic inhibitors. J. Mol. Biol. **328**, 109-118

16 Frese, K. K. and Tuveson, D. A. (2007) Maximizing mouse cancer models. Nature Reviews Cancer **7**, 645-658

17 Dano, K., Nielsen, L. S., Moller, V. and Engelhart, M. (1980) Inhibition of a plasminogen activator from oncogenic virus-transformed mouse cells by rabbit antibodies against the enzyme. Biochim. Biophys. Acta. **630**, 146-151

18 Klinghofer, V., Stewart, K., McGonigal, T., Smith, R., Sarthy, A., Nienaber, V., Butler, C., Dorwin, S., Richardson, P., Weitzberg, M., Wendt, M., Rockway, T., Zhao, X., Hulkower, K. I. and Giranda, V. L. (2001) Species specificity of amidine-based urokinase inhibitors. Biochemistry **40**, 9125-9131

19 Hansen, M., Wind, T., Blouse, G. E., Christensen, A., Petersen, H. H., Kjelgaard, S., Mathiasen, L., Holtet, T. L. and Andreasen, P. A. (2005) A urokinase-type plasminogen activator-inhibiting cyclic peptide with an unusual P2 residue and an extended protease binding surface demonstrates new modalities for enzyme inhibition. J. Biol. Chem. **280**, 38424-38437

20 Zhao, G., Yuan, C., Wind, T., Huang, Z., Andreasen, P. A. and Huang, M. (2007) Structural basis of specificity of a peptidyl urokinase inhibitor, upain-1. J. Struct. Biol. **160**, 1-10

21 Kvassman, J. O., Verhamme, I. and Shore, J. D. (1998) Inhibitory mechanism of serpins: loop insertion forces acylation of plasminogen activator by plasminogen activator inhibitor-1. Biochemistry **37**, 15491-15502

22 Olson, S. T., Bock, P. E., Kvassman, J., Shore, J. D., Lawrence, D. A., Ginsburg, D. and Bjork, I. (1995) Role of the catalytic serine in the interactions of serine proteinases with protein inhibitors of the serpin family. Contribution of a covalent interaction to the binding energy of serpin-proteinase complexes. J. Biol. Chem. **270**, 30007-30017

23 Koivunen, E., Wang, B., Dickinson, C. D. and Ruoslahti, E. (1994) Peptides in cell adhesion research. Methods Enzymol. **245**, 346-369

24 Scott, J. K. and Smith, G. P. (1990) Searching for peptide ligands with an epitope library. Science **249**, 386-390

25 Jensen, J. K., Wind, T. and Andreasen, P. A. (2002) The vitronectin binding area of plasminogen activator inhibitor-1, mapped by mutagenesis and protection against an inactivating organochemical ligand. FEBS Lett **521**, 91-94

26 Wind, T., Jensen, J. K., Dupont, D. M., Kulig, P. and Andreasen, P. A. (2003) Mutational analysis of plasminogen activator inhibitor-1. Eur. J. Biochem. **270**, 1680-1688

27 Larsen, K. S., Ostergaard, H., Bjelke, J. R., Olsen, O. H., Rasmussen, H. B., Christensen, L., Kragelund, B. B. and Stennicke, H. R. (2007) Engineering the substrate and inhibitor specificities of human coagulation Factor VIIa. Biochem. J. **405**, 429-438

28 Diamond, S. (2007) Methods for mapping protease specificity. Curr. Opin. Chem. Biol. **11**, 46-51

29 Ladner, R. C., Sato, A. K., Gorzelany, J. and de Souza, M. (2004) Phage display-derived peptides as therapeutic alternatives to antibodies. Drug Discov. Today **9**, 525-529

30 Schwede, T., Kopp, J., Guex, N. and Peitsch, M. C. (2003) SWISS-MODEL: An automated protein homology-modeling server. Nucleic Acids Res. **31**, 3381-3385

FIGURE LEGENDS

Figure 1 The effect of mupain-1 on the plasminogen activation activity of muPA

(A) MuPA (0.25 nM) was incubated for 15 min without (black circle) or with 0.1 μM (open circle), 0.25 μM (black triangle), 0.5 μM (open triangle), 1 μM (black square), 2.5 μM (open square), 5 μM (black diamond), 10 μM (open diamond) mupain-1 after which plasminogen (0.5 μM) and S-2251 (500 μM) were added. The reaction was followed spectrophotometrically at 405 nm. (**B**) Effect on cell surface-associated plasminogen activation. Aliquots of WEHI-3 cell suspension (10^7 cells/ml) that had been saturated with muPA were incubated at room temperature for 15 min without addition (open circle) or in the presence of 0.1 μM (black triangle), 1 μM (open triangle), 5 μM (black square), 20 μM (open square), 100 μM (black diamond) mupain-1 or 100 μM mupain-1(R6A) (open diamond). Cells without muPA (black circle) served as a negative control. Plasminogen and the fluorogenic plasmin substrate VLK-AMC were added and fluorescence was measured over time.

Figure 2 Association and dissociation curves for mupain-1-D1D2 and mupain-1 peptide binding to muPA, as studied by surface plasmon resonance

A monoclonal anti-muPA antibody was immobilised on a CM5 sensor chip in a BIACORE T100. Hundred nM muPA was injected to a capture level of ~250 RU. Mupain-1-D1D2 (0-25 μM) or mupain-1 (0-5 μM) were injected and the association and dissociation time courses followed. The kinetic parameters k_{on}, k_{off}, and K_D were estimated by global fitting to a 1:1 binding model, using the BIACORE T100 evaluation software (Table 2).

Figure 3 Effect of alanine substitutions of specific residues in muPA on the binding of mupain-1

(A) Phage particle ELISA. Media from HEK293T cells transfected with the corresponding cDNA's were used directly in the assay. uPA was captured in Ni-NTA coated wells. After removal of excess muPA, mupain-1 phage particles were allowed to bind and subsequently detected by a HRP-conjugated anti-M13 antibody. Background signals from wells without muPA were subtracted before the signals were normalized to the actual capture level of muPA in the wells and the signal obtained with wt muPA.

(B) BIACORE binding analysis. muPA variants from conditioned media from HEK293T were captured on a monoclonal anti-muPA antibody which was immobilised on a CM5 chip and the binding of mupain-1-D1D2 to muPA was monitored. Background signals from binding analysis without muPA has been subtracted and the data are normalized to the binding signal obtained for wt.

Figure 4 A three-dimensional model of muPA and the binding site for mupain-1

Shown are ribbon (A) and surface (B) representation of a three-dimensional model of muPA that was generated using SWISSmodel [30]. It is based on a sequence alignment of the protease domain of huPA and muPA and the X-ray crystal structure in Zhao et al. 2007 [20]. The orientation of the structures in A and B is the same. The identification of mupain-1 binding residues in muPA was based on mupain-1 phage particle ELISA and SPR analysis using mupain-1-D1D2. **(A)** the active site of muPA and its surroundings. Residues of the catalytic triad are labelled by identity as well as surface exposed loops which are coloured green. The side chains of the residues involved in binding of mupain-1 are depicted in red while those having no or only weak effect on binding of mupain-1 when changed individually to alanine are depicted in blue. Amino acids are numbered according to

chymotrypsin. **(B)** mupain-1 binding residues in muPA, as based on phage particle ELISA and SPR binding analysis. Alanine substitutions of the residues coloured red resulted in pronounced loss of binding of mupain-1. Alanine substitutions of the residues coloured blue showed no or only a weak reduction in binding of mupain-1.

Figure 5 Stability of mupain-1 in mouse serum or fetal bovine serum

Mupain-1 (400 μM) was incubated with 77% mouse serum **(A)** or 77% fetal bovine serum **(B)** for 0, 1, 2, or 20 hours. The serum was then acid treated to inactivate the α_2-macroglobulin. Aliquots of incubation mixtures, corresponding to different initial concentrations of mupain-1 added to the serum, were then mixed with 4 nM muPA. The remaining activity of muPA was determined by an S-2444 assay. A background achieved with serum without mupain-1 has been subtracted from all samples. In all cases serum constitutes 2.5% of the total reaction volume in the assay.

Table 1 Mupain-1 is a competitive inhibitor of muPA activity

Initial rates of muPA-catalysed hydrolysis of varying concentrations of S-2444 in the presence of varying concentrations of mupain-1 were estimated by monitoring the time course of the absorbance at 405 nm. The apparent K_m values (K_m^{app}) and the apparent V_{max} (V_{max}^{app}) values were determined by non-linear regression analysis of rate-substrate data pairs on the basis of Equation 1. Indicated are means and S.D.s for two independent determinations.

[mupain-1] (μM)	K_m^{app} (mM)	V_{max}^{app} (10^{-8} M/s)
0	2.6 ± 0.2	3.9 ± 0.2
0.250	3.0 ± 0.4	3.5 ± 0.2
0.500	3.9 ± 0.6	3.7 ± 0.3
1	5.5 ± 0.4	3.5 ± 0.2
2	8.6 ± 0.5	3.4 ± 0.1

Table 2 K_D values for mupain-1-muPA binding

A monoclonal anti-muPA antibody was immobilised on a CM5 sensor chip in a BIACORE T100. Hundred nM muPA (100 nM) was injected. After having obtained a stable muPA capture level, different concentrations of mupain-1 peptide (0-5 μM) or mupain-1-D1D2 (0-25 μM) were injected and the association and dissociation time courses followed. In the inverse experimental setup, mupain-1-D1D2 was immobilised, muPA (0-15 μM) was injected and association and dissociation was followed over time. The data was fitted to the simple exponential equations for association and dissociation and the apparent rate of association and dissociation were determined. Data are reported as means ± S.D. for the indicated number of experiments.

On the solid phase	In the fluid phase	k_{on} ($\mu M^{-1}s^{-1}$)	k_{off} (s^{-1})	K_D (μM)
MuPA	Mupain-1 peptide	0.16 ± 0.04 (4)	0.050 ± 0.020 (4)	0.33 ± 0.11 (4)
MuPA	Mupain-1-D1D2	0.053 ± 0.038 (3)[1]	0.066 ± 0.033 (3)	14 ± 2.3 (3)[1]
Mupain-1-D1D2	MuPA	0.018 ± 0.002 (3)	0.252 ± 0.004 (3)	14 ± 0.9 (3)

[1]Significantly different from the corresponding value for mupain-1 peptide ($p < 0.01$)

Table 3 Reactivity of mupain-1 toward serine proteases related to murine uPA

Kinetic parameters were determined in assays with the indicated chromogenic substrates in HBS with 0.1% BSA at pH 7.4 and at 37°C, except for human fVIIa, which was assayed in TBS at pH 8.1. The reported inhibition constants were determined from the combined data of three independent experiments and global evaluation by Equation 4. Data are reported as the fitted value ± S.D. after correction for the competitive effect of the chromogenic substrate.

Protease	Substrate	K_m (μM)	K_i (μM)
Murine uPA	S-2444	1190 ± 0.3 (3)	0.412 ± 0.180 (7)
Murine tPA	S-2765	187 ± 13 (3)	>580[1]
Murine plasmin	S-2366	179 ± 7 (3)	>640[1]
Murine thrombin	S-2238	37 ± 9 (3)	>370[1]
Murine β-trypsin	S-2222	55 ± 8 (3)	45 ± 3 (3)[1]
Murine aPC	S-2366	584 ± 39 (3)	>730[1]
Murine fIXa	Spectrozyme^{fIXa}	>1250[2]	>675[1]
Murine fXa	S-2765	78 ± 23 (3)	>180[1]
Murine plasma kallikrein	S-2302	116 ± 40 (3)	>650[1]
Human uPA	S-2444	85 ± 0.3 (3)	>870[1]
Human tPA	S-2288	331 ± 0.1 (3)	>710[1]
Human plasmin	S-2403	106 ± 1 (3)	>620[1]
Human thrombin	S-2238	17.3 ± 0.9 (3)	>350[1]
Human aPC	S-2366	711 ± 0.4 (3)	>950[1]
Human fVIIa	Spetrozyme^{fVIIa}	>500[2] (3)	>680[1]
Human fXa	S-2765	101 ± 0.5 (3)	>680[1]
Human plasma kallikrein	S-2302	300 ± 0.3 (3)	>680[1]
Bovine β-trypsin	S-2222	60.0 ± 0.2 (3)	20.7 ± 0.5 (3)[1]

[1]Significantly different from the corresponding value for wt mupain-1 ($p < 0.01$).

[2]Saturating levels of substrate could not be reached in the absence of tissue factor and thus 500 μM represents a lower limit for the K_m value under the tested conditions.

Table 4 Alanine scanning analysis of the importance of individual mupain-1 residues required for muPA inhibition

The K_i values for inhibition of muPA by the indicated peptides were determined by an assay with the chromogenic substrate S-2444, in HBS with 0.1% BSA at a temperature of 37°C. The reported inhibition constants were determined from the combined data of the indicated number of independent experiments and global evaluation by Equation 4. Data are reported as means ± S.D for the indicated number of experiments.

The binding of the indicated peptides to muPA was characterised by the use of surface plasmon resonance with a BIACORE T100 instrument equipped with a CM5 chip coupled with a monoclonal antibody against the A-chain of muPA. After coating with 250 RU of muPA, the peptide variants were passed over the chip in various concentrations between 0 μM and 5 μM at 25°C. The K_D values were determined from the concentration dependence of the steady state levels (Equation 5). The table shows means and standard deviations for the indicated number of independent determinations.

Sequence	Peptide name	Chemical peptide	Fusion protein	Chemical peptide
		K_i (μM)	K_i (μM)	K_D (μM)
CPAYSRYLDC	Mupain-1 wt	0.41 ± 0.18 (7)	5.20 ± 0.10 (3)	0.33 ± 0.11 (4)[2]
CPLYNRMIGC	Mupain-2	n.d.[1]	13.2 ± 0.4 (3)	n.d.[1]
CAAYSRYLDC	Mupain-1 P2A	13 ± 0.4 (4)[2]	n.d.[1]	4.9 ± 0.26 (2)[2]
CPAASRYLDC	Mupain-1 Y4A	67 ± 1.9 (4)[2]	n.d.[1]	22.6 ± 12.8 (4)[2]
CPAYARYLDC	Mupain-1 S5A	57 ± 1.0 (4)[2]	480 ± 13 (3)[2]	45.2 ± 4.20 (2)[2]
CPAYSAYLDC	Mupain-1 R6A	> 830 (2)[2]	280 ± 18 (3)[2]	>300 (4)[2]
CPAYSRALDC	Mupain-1 Y7A	4.0 ± 0.05 (4)[2]	n.d.[1]	2.5 ± 0.5 (3)
CPAYSRYADC	Mupain-1 L8A	1.4 ± 0.03 (4)[2]	n.d.[1]	0.83 ± 0.15 (2)
CPAYSRYLAC	Mupain-1 D9A	0.89 ± 0.02 (4)	n.d.[1]	0.57 ± 0.06 (2)
SPAYSRYLDS	Linearised mupain-1	> 430	n.d.[1]	>300[2]
CSWRGLENHRMC	Upain-1	n.d.[1]	1200 ± 93	n.d.[1]

[1]n.d., not determined

[2]Significantly different from the corresponding value for wt mupain-1 ($p < 0.01$).

Table 5 Effects of grafting amino acid residues from muPA onto huPA on the K_m values for hydrolysis of S-2444 and K_i values for inhibition by mupain-1

Kinetic parameters were determined in HBS with 0.1% BSA at pH 7.4 and at 37°C with conditioned media from HEK293T cells transfected with the corresponding huPA cDNAs. The reported inhibition constants were determined from the combined data of three independent experiments and global evaluation by Equation 4.

huPA variant	K_m (mM)	V_{max} (10^{-7} M/s)	K_i (μM)	K_D (μM)
wt	0.31 ± 0.03 (3)	2.0 ± 0.6 (3)	> 550	n.b.[1]
V41K	0.47 ± 0.07 (3)	2.6 ± 0.3 (3)	> 630	n.b.[1]
H99Y	0.61 ± 0.11 (3)	2.3 ± 0.3 (3)	15.3 ± 2.0 (3)	12.0 ± 4.7 (3)
Q192K	0.76 ± 0.14 (3)	4.0 ± 0.6 (3)	> 600	n.b.[1]
V41K/H99Y	1.04 ± 0.21 (3)	4.0 ± 0.6 (3)	6.9 ± 1.0 (3)	6.0 ± 2.3 (3)
V41K/Q192K	1.20 ± 0.27 (3)	3.7 ± 0.9 (3)	> 710	n.b.[1]
H99Y/Q102K	1.80 ± 0.28 (3)	4.0 ± 0.6 (3)	9.4 ± 1.3 (3)	12.2 ± 5.7 (3)
V41K/H99Y/Q192K	3.35 ± 0.78 (3)	3.2 ± 0.6 (3)	3.6 ± 0.8 (3)	4.2 ± 1.3 (3)

[1]n.b., no binding of mupain-1 at a concentration of 50 μM

Table 6 Amino acid residue variation among related serine proteases in the position critical for binding to muPA

If no residue is indicated, the protease does not have that position filled. Residue numbers are according to the chymotrypsin template numbering. The alignment is that given by Mackman et al. [10] or a sequence-based alignment, performed with ClustalW (www.ebi.ac.uk/Tools/clustalw/) in the case of trypsin, aPC and the murine proteases.

Proteinase	Amino acid residue		
	41	99	192
Human uPA	V	H	Q
Mouse uPA	K	Y	K
Human tPA	L	Y	Q
Mouse tPA	L	Y	Q
Human plasmin	F	-	Q
Mouse plasmin	F	-	Q
Human thrombin	L	L	E
Mouse thrombin	L	L	E
Human fVIIa	L	T	K
Mouse fVIIa	L	I	K
Human fXa	F	Y	Q
Mouse fXa	F	Y	Q
Human trypsin	F	L	Q
Mouse trypsin	F	L	Q
Bovine trypsin	F	L	Q
Human plasma kallikrein	L	G	K
Mouse plasma kallikrein	L	G	K

Figure 1

A

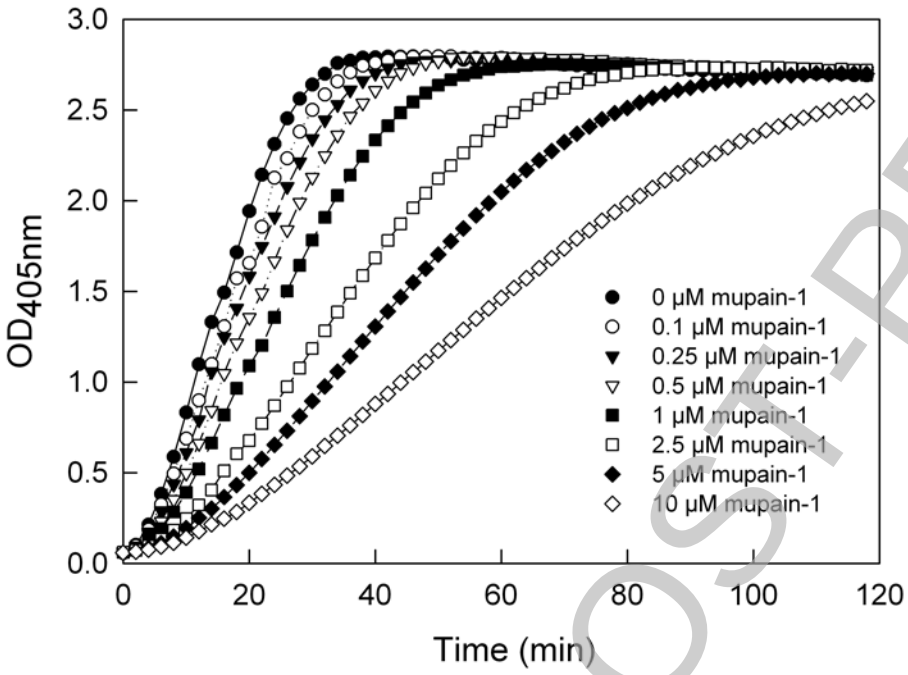

B

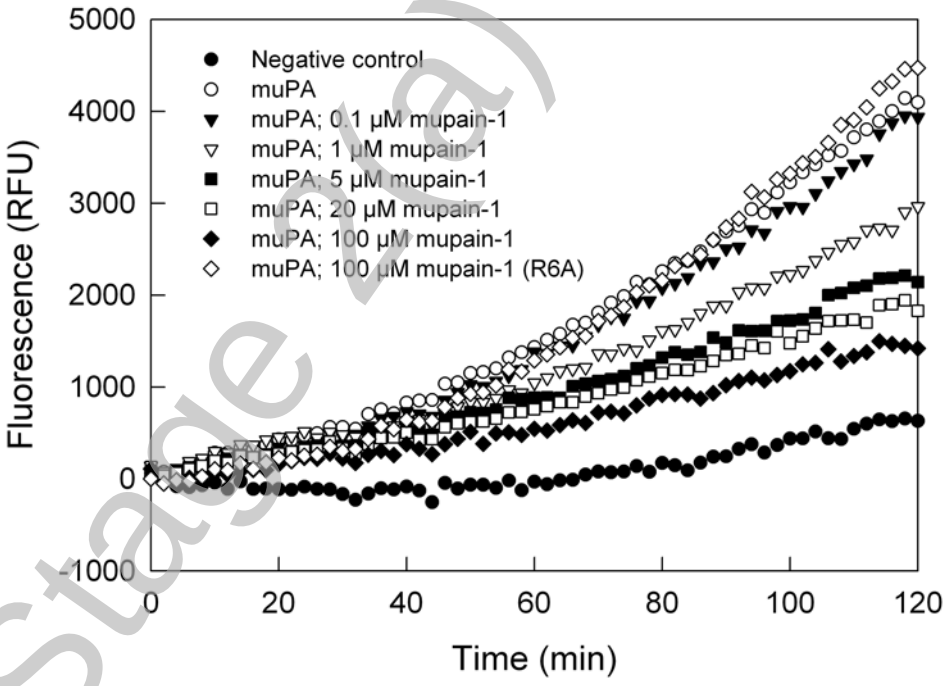

Biochemical Journal Immediate Publication. Published on 04 Mar 2008 as manuscript BJ20071646

Figure 2

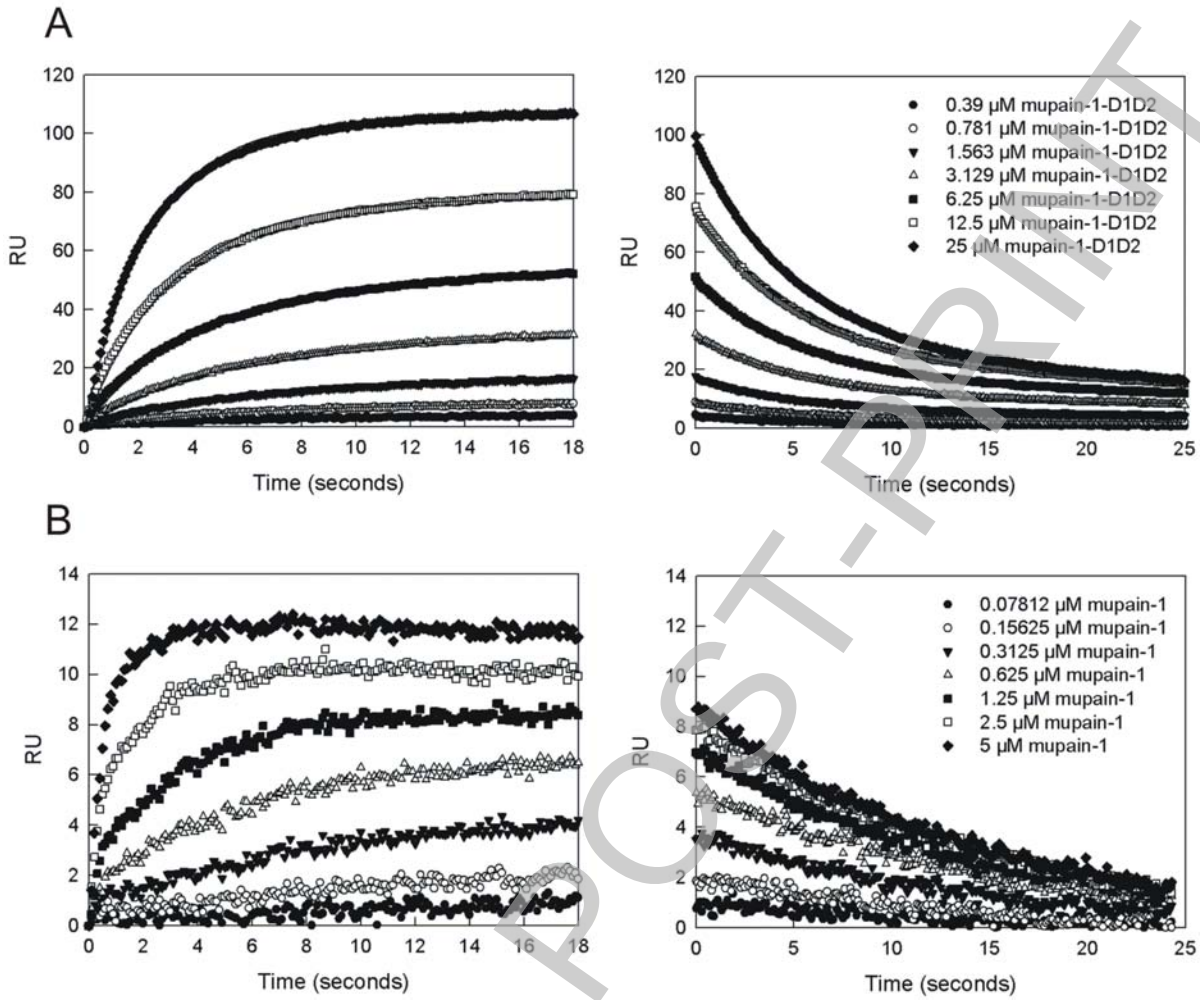

Figure 3

A

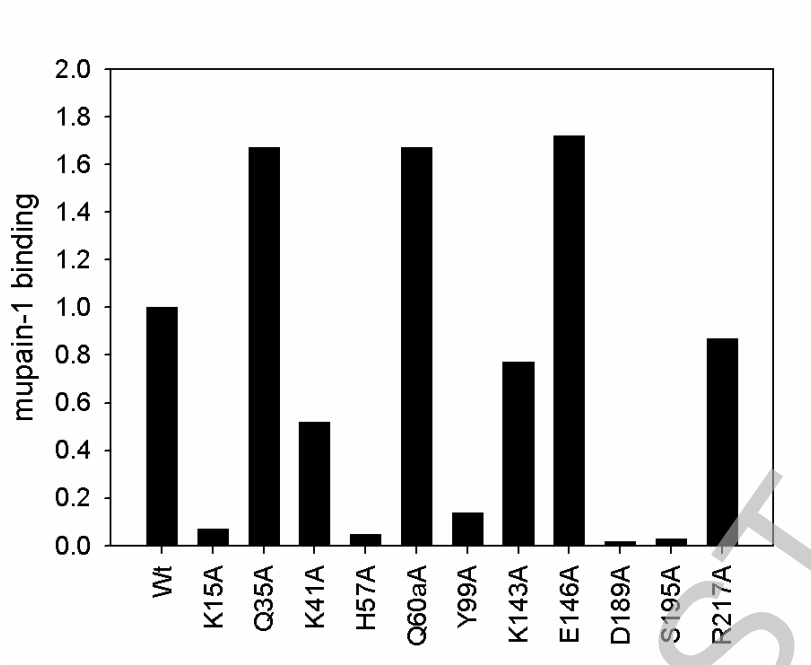

B

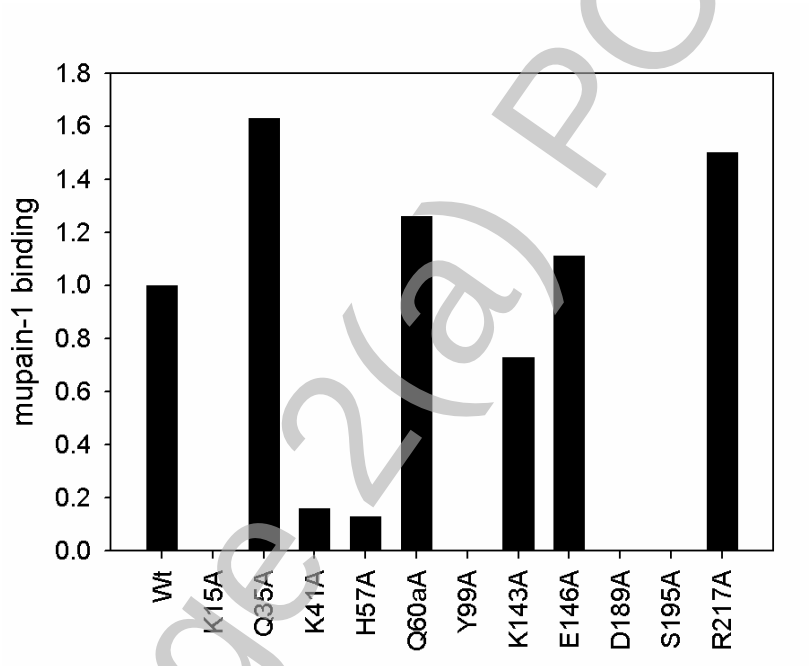

Biochemical Journal Immediate Publication. Published on 04 Mar 2008 as manuscript BJ20071646

Figure 4

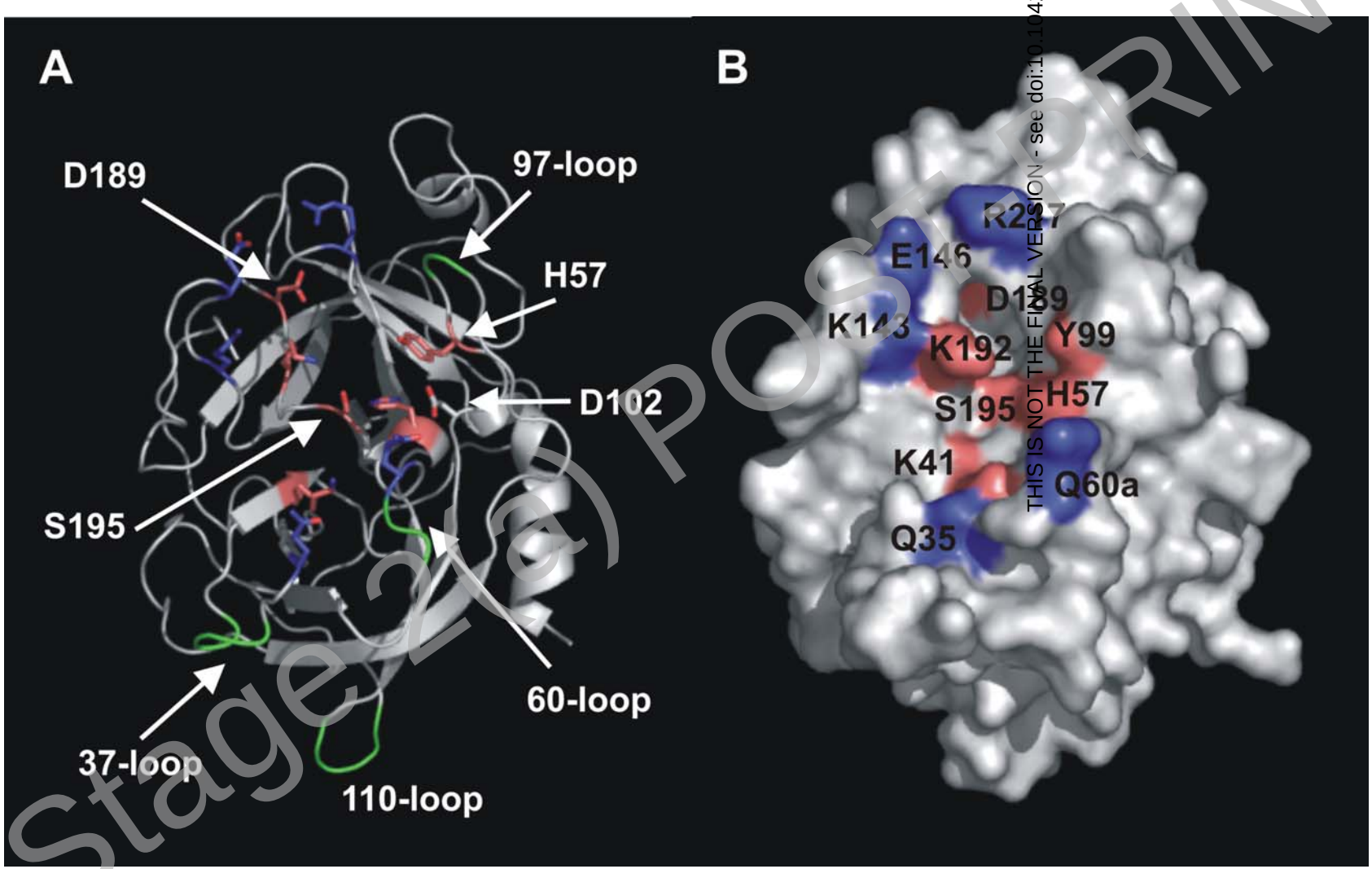

Figure 5

A

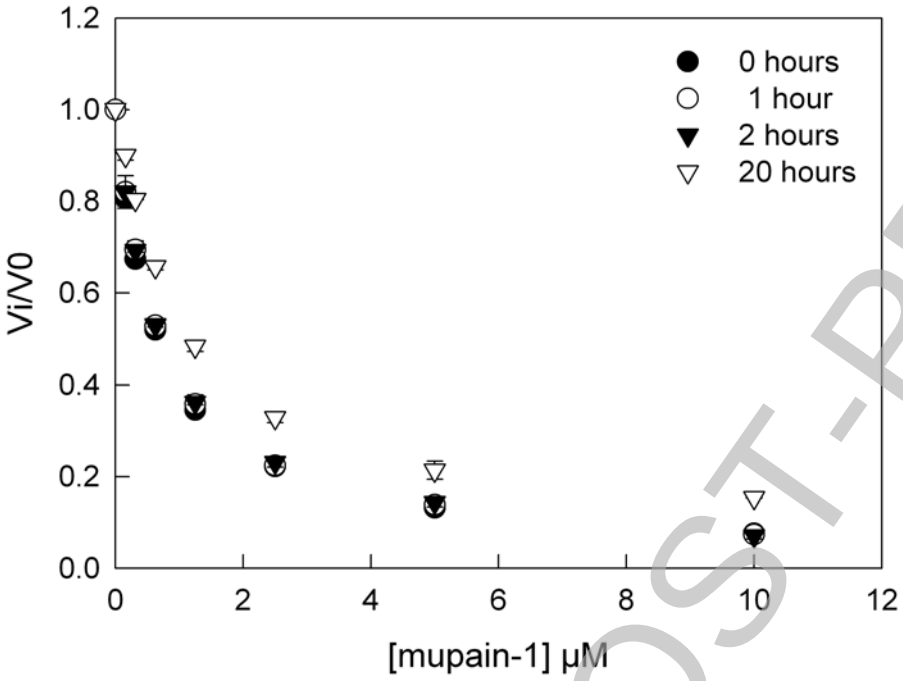

B